Journal of Nuclear Materials 508 (2018) 203–211

Contents lists available at ScienceDirect

Journal of Nuclear Materials

journal homepage: www.elsevier.com/locate/jnucmat

Immobilisation of Prototype Fast Reactor raffinate in a barium borosilicate glass matrix

Paul G. Heath*, Claire L. Corkhill, Martin C. Stennett, Russell J. Hand, Kieran M. Whales, Neil C. Hyatt

Immobilisation Science Laboratory, Sir Robert Hadfield Building, Mappin Street, The University of Sheffield, Sheffield S1 3JD, United Kingdom

ARTICLE INFO

Article history:
Received 20 December 2017
Received in revised form
2 May 2018
Accepted 5 May 2018
Available online 7 May 2018

Keywords:
Amorphous materials
Waste immobilisation
Mechanical properties

ABSTRACT

The vitrification of Dounreay Prototype Fast Reactor (PFR) Raffinate in a barium borosilicate glass matrix was investigated, with the aim of understanding process feasibility and the potential benefits over the current baseline of cement encapsulation. Laboratory scale glass melts demonstrated the production of homogeneous glasses incorporating at least 20 wt% simulant PFR waste (on an oxides basis), with no detectable crystalline accessory phases. The hardness and indentation fracture toughness of the simulant PFR waste glasses were determined to be comparable to those of current UK high level waste glass formulations. The normalised dissolution rate of boron from the simulant PFR glasses was determined to be 3×10^{-2} g m^{-2} d^{-1}, in 18.2 MΩ water at 90 °C and surface area/volume ratio of 1500 m^{-1}, only a factor of two greater than the French SON-68 simulant high level waste glass, under comparable conditions. Consequently, the simulant PFR waste glasses show considerable promise for meeting envisaged waste acceptance criteria for geological disposal. Overall, the superior stability of vitrified PFR wasteforms could enhance the safety case for long term near surface storage of radioactive wastes, mandated by current Scottish Government policy.

1. Introduction

The Prototype Fast Reactor (PFR) was the UK's second fast reactor and operated between 1974 and 1994, utilising a high plutonium content mixed oxide fuel (MOx) with a molten sodium coolant [1]. Spent fuel from the PFR was reprocessed on the Dounreay site by dissolution in nitric acid to recover the reusable fissile material. This process yielded approximately 200 m^3 of an aqueous radioactive liquor, known as PFR raffinate [2]. The PFR raffinate contains the majority of the radioactive material and fission products produced during the operation of the PFR reactor and on the Dounreay site as a whole [3]. Since the reprocessing of PFR fuel was completed in 1996, the waste raffinate has been stored in underground tanks on the Dounreay site. Having spent a decade in storage, PFR raffinate was reclassified as Intermediate Level Waste in 2004, ostensibly due to its low heat output [4].

The conditioning of PFR raffinate into a passively safe, waste-form is identified as a priority in the Dounreay Site Restoration Plan [5]. A best practical environmental option assessment, undertaken by the UKAEA, proposed neutralisation and cementation of the raffinate as the reference waste management strategy [6]. For this waste treatment option to be implemented, a new facility (to be known as D3900) is required, the construction of which is yet to begin at the time of writing.

Although laboratory studies have demonstrated that cement-encapsulated *inactive* raffinate has physical properties comparable to those of other cemented ILW streams (e.g. viscosity, initial setting time, bleed water), PFR raffinate has a specific activity 20 times greater than other encapsulated ILW streams [2,3,7,8]. The high concentration of ^{137}Cs in PFR raffinates, the porous nature and poor immobilisation of Cs observed in cementitious systems, may limit the ability of cement to retain the radioactive inventory of PFR [2,9–11]. It is not yet certain that environmental release rates from a cemented PFR raffinate wasteform will be within permitted limits over the relevant lifetime of the wasteform, particularly given the policy of the Scottish Government for long term near-surface storage at a coastal location, as in the case of Dounreay [12,13].

An issue that may be even more significant to safe interim storage of conditioned PFR raffinate is the high specific activity of

* Corresponding author.
E-mail address: paul.heath@georoc.co.uk (P.G. Heath).

https://doi.org/10.1016/j.jnucmat.2018.05.015
0022-3115/

the wastes and their significant alpha emitting component (β/γ = 346 TBq m^{-3}, α = 3.21 TBq m^{-3}) [2]. It is known that the radiolysis of cementitious water will produce H_2, while the presence of significant nitrate concentrations in the waste (300–500 g l^{-1}) and alpha activity will also result in the formation of O_2 and NO_x [14–17]. These combined factors will increase the rate of gas generation when compared to existing UK ILW waste packages. As a result, these reactions could be expected to introduce significant complexities to the long-term management of cemented PFR raffinate waste packages through the need to monitor, vent and dissipate gases form the waste packages.

It should be noted that the near-surface storage policy was introduced after the strategic decision to encapsulate PFR raffinates in a cement wasteform. In its response to the Scottish Government consultation on higher activity wastes, the Committee on Radioactive Waste Management (CoRWM) highlighted that certain wastes from the Dounreay site were "*never likely to be suitable for near surface disposal and therefore greater efforts need to be made in the interest of safety, security and intergenerational equity to find a permanent solution for this waste*" [12].

The current investigation aims to demonstrate, in principle, an alternative processing option for PFR raffinate, which could enhance the safety case for long term near-surface storage and address the concerns of CoRWM. A derivative of the barium borosilicate glass, G73, previously investigated as a matrix for the immobilisation of UK ILWs arising at Magnox decommissioning sites [18–21], is here investigated as a disposal matrix for PFR raffinate, the composition of which incorporates ca. 7 wt% SO_3. Barium borosilicate glasses, such as G73, are reported to have a high aqueous durability and the presence of Ba is known to increase the solubility of sulphate species, which inhibits the formation of water soluble "yellow phase" salts [18–23]. We present an analysis of the composition, amorphous nature, aqueous durability, thermal behaviour and mechanical properties of vitrified PFR raffinate with waste loadings of 10 wt%, 15 wt% and 20 wt% (oxide basis), in a barium borosilicate glass. The results are discussed with reference to the potential benefits of PFR raffinate vitrification compared to cementation.

2. Materials and experimental

2.1. Materials

2.1.1. Raffinate simulant

The inactive surrogate for PFR raffinate was formulated on the assumption that the waste would be treated using an evaporation or calcination step to produce a solid calcine prior to vitrification. The composition was thus formulated using the data available on the average composition of four PFR tanks at the Dounreay site [6]. The chemical composition of model PFR raffinate is provided in Table 1. The solids content of the raffinate calcine was calculated based on the reported elemental values in the raffinate (ppm) and then converted to their oxide form, which is reported in Table 2.

Some variation from the reported raffinate composition was necessary when batching the simulant. For example, for reasons of practicality, elements with concentrations <15 ppm were excluded (Ag, As, Cm, Dy, Eu, Gd, Ge, Hg, Ho, In, Nb, Np, P, Pb, Pd, Rb, Rh, Sb, Se, Sn and Tc). One exception was Pd, which was present at a concentration of ~150 ppm in the waste stream. This was excluded on grounds of cost, for this preliminary study, and its known propensity to exist as an insoluble noble metal in glass melts [24].

The omission of the elements noted above accounted for <2.8 wt% of the mass of the total waste stream. Radioactive elements with concentrations >15 ppm were substituted by relevant concentrations of inactive surrogates (Ce for U and Sm for Am).

Table 1
Average composition of PFR raffinate as characterised in Ref. [6]. (Brackets) indicate where the use of an appropriate inactive simulant was applied. The right-hand columns identifies elements excluded from the simulant based on either their low concentration in the raffinate or on an economic basis.

Included in Simulant (surrogate element used)		Excluded from Simulant	
Element	ppm	Element	ppm
Na	9711	Rh	15
Cu	8725	Cm	4
Fe	3837	Nb	3.5
Zn	3566	Dy	2.4
Cd	2540	Ag	<1.3
S	1351	As	<13
Ni	1277	Co	<0.4
Cr	669	Ge	<1.3
Cs	509	Hg	<0.3
Nd	462	Ho	<1.3
Am (Sm)	405	In	<4
Al	350	Np	<13
Ce	304	P	<2.7
U (Ce)	168	Pb	<1.1
La	163	Rb	<1.3
Pr	158	Sb	<1.3
Mo	154	Se	<1.3
Pd	150	Sn	<0.3
Ca	138	Tc	<1.3
Sm	123	Eu	15
Y	112	Gd	15
Te	74	Pd	150
Sr	60		
Mn	45		
Ru	60		
Ba	39		
Ti	36		
Total	35,186	Total	205

2.1.2. Glass preparation

Three glasses were synthesised and characterised in this study. These glasses were based on a derivative of the G73 barium-silicate base glass composition (referred to here as G73, for simplicity), which was previously developed [18–21], with PFR raffinate simulant incorporated at 10 wt%, 15 wt% and 20 wt% waste loading (on an oxides basis). These glasses are identified as G73-10, G73-15 and G73-20, respectively. The base glass composition, presented in Table 2 for reference, is identified as G73-00.

Glasses were produced from batch chemicals to provide 250 g of glass. The components of the raffinate simulant were batched in either their oxide or carbonate forms according to their molar proportions to obtain the specified waste loading. The following analytical grade chemicals were used for batching; $Al(OH)_3$, $Na_2B_4O_7.10H_2O$, $BaCO_3$, $CaCO_3$, CdO, CeO_2, $Cr(NO_3)_3.9H_2O$, Cs_2CO_3, CuO, Fe_2O_3, La_2O_3, Mn_2O_3, MoO_3, Na_2CO_3, Nd_2O_3, $NiCO_3$, Pr_6O_{11}, RuO_2, Na_2SO_4, SiO_2, Sm_2O_3, $SrCO_3$, TeO_2, TiO_2, Y_2O_3 and ZnO. The batched powders were heated in mullite crucibles with stirring to 1200 °C at 10 °C min^{-1} and held at temperature for 3 h. The glasses were poured into blocks and annealed at 500 °C for 1 h before cooling to 25 °C at 1 °C min^{-1}. Glass monoliths were prepared for SEM-EDX, Vickers hardness testing and fracture toughness testing to a 0.25 μm finish by successive grinding and polishing with SiC grit papers and diamond pastes. Powder samples were prepared using a hardened steel ring and puck mill. The sub-75 μm size fraction was collected for use in XRD and XRF analysis and the 75–150 μm size fraction was collected for use in aqueous durability experiments and prepared according to ASTM standard C 1285–02 [25].

Table 2
Compositions of base glass, simulant calcined PFR raffinate and glasses produced. Compositions of glasses provided both as batched and as measured by XRF (boron analysis via dissolution in HF and ICP-AES). *Note glasses were batched to 100 wt%; discrepancies reported result from rounding to 2 d.p.

Component (wt%)	G73-00 Base Glass	PFR Calcine	G73-10		G73-15		G73-20	
			Batch	Meas.	Batch	Meas.	Batch	Meas.
SiO_2	42.0	0.00	37.80	34.29	35.70	33.4	33.60	32.58
BaO	42.0	0.09	37.81	41.21	35.71	41.61	33.62	38.61
Fe_2O_3	6.00	11.68	6.57	7.88	6.85	7.78	7.14	7.56
CaO	5.00	0.41	4.54	4.55	4.31	4.54	4.08	4.40
Na_2O	2.50	27.88	5.04	1.64	6.31	2.38	7.58	3.30
CuO	0	26.26	2.63	2.83	3.94	3.98	5.25	5.05
B_2O_3	2.00	0.00	1.80	0.46	1.70	0.56	1.60	0.46
ZnO	0	9.45	0.95	1.08	1.42	1.55	1.89	1.93
CdO	0	6.18	0.62	0.74	0.93	1.05	1.24	1.35
SO_3	0	7.18	0.72	0.72	1.08	0.79	1.44	0.86
Al_2O_3	0.50	1.41	0.59	0.86	0.64	0.85	0.68	1.2
NiO	0	3.46	0.35	0.55	0.52	0.71	0.69	0.86
Cr_2O_3	0	2.08	0.21	0.48	0.31	0.56	0.42	0.66
Cs_2O	0	1.15	0.12	0.36	0.17	0.42	0.23	0.52
Nd_2O_3	0	1.15	0.12	0.15	0.17	0.00	0.23	0.23
Sm_2O_3	0	0.30	0.03	0.10	0.05	0.14	0.06	0.19
CeO_2	0	0.97	0.10	0.05	0.15	0.10	0.19	0.12
MoO_3	0	0.49	0.05	0.06	0.07	0.08	0.10	0.09
Y_2O_3	0	0.30	0.03	0.03	0.05	0.05	0.06	0.06
La_2O_3	0	0.04	0.00	0.03	0.01	0.00	0.01	0.04
Pr_6O_{11}	0	0.04	0.00	0.04	0.01	0.06	0.01	0.09
RuO_2	0	0.17	0.02	0.00	0.03	0.00	0.03	0.00
SrO	0	0.15	0.02	0.6	0.02	0.12	0.03	0.07
TeO_2	0	0.20	0.02	0.00	0.03	0.00	0.04	0.00
TiO_2	0	0.13	0.01	0.00	0.02	0.00	0.03	0.00
Mn_2O_3	0	0.14	0.01	0.08	0.02	0.08	0.03	0.09
	100	–	100.13	98.795	100.20	100.81	100.26	100.32

2.2. Characterisation

2.2.1. Glass characterisation

X-ray Fluorescence (XRF) analysis was performed using a Phillips PW2404 XRF Axios instrument to obtain compositional data. B_2O_3 content was determined by dissolution of glass powder in HF followed by analysis of leachate using a Perkin-Elmer Optima 5300 dual view Inductively Coupled Plasma Atomic Emission Spectroscopy (ICP-AES). The density of the glass wasteforms was measured using a <75 μm powder, using an AccuPyc 1340 II helium pycnometer with the following analysis regime; 200 purges of the chamber followed by 50 cycles using an equilibration rate of 35 Pa min^{-1} at 25 °C in a 1 cm^3 chamber and a fill pressure of 86.2 KPa. Scanning Electron Microscopy was performed using a JEOL JSM 6400 SEM with an accelerating voltage of 20 kV and a working distance of 15 mm. Concurrent Energy Dispersive X-ray Spectroscopy (EDX) was acquired (INCA, Oxford Instruments). Additionally, an FEI Quanta 200 F SEM was utilised for high resolution imaging, using an accelerating voltage of 30 kV and working distance of 10 mm. Concurrent Energy Dispersive X-ray analysis was performed (Genesis EDX).

2.2.2. Thermal and mechanical properties

The glass liquidus temperature for each sample was measured by placing a 20 cm long mullite boat, filled with sub-75 μm glass powder, into a tube furnace. The samples were left to equilibrate at 1200 °C for 24 h and the temperature gradient along the length of the boat at 5 mm intervals was measured using a retractable thermocouple. The boats were removed and rapidly quenched in air. The point of crystallisation was measurable to within 1 mm by optical examination of the crucibles and this was then correlated with the associated temperature to estimate the liquidus temperature. Alterations in chemical composition resulting from crucible corrosion were not accounted for, nor were the phases produced analysed. As the purpose of this test was to check if the point of crystallisation was below 1100 °C, and the contaminants from crucible corrosion are likely to lower this value, the results presented are considered meaningful in this context.

The Vickers hardness indentation method was used to determine both hardness (H_v) and the indentation fracture toughness (K_c) following the procedure described by Connelly et al. [26]. Indentation was performed on a Mitutayo HM-101. Sixty indents were made at each of three indentation loadings; 0.98 N, 1.96 N and 2.94 N (twenty indents at each force per sample, error ± 0.02 N). The load was held for 20 s. Samples were left for 24 h prior to analysis using optical microscopy. The Vickers hardness (Hv) in Pa and the Fracture Toughness (Kc) was calculated using Equations (1) and (2) respectively:

$$H_v = \frac{1.854P}{(2a)^2} \quad (1)$$

$$K_C = \frac{0.0824P}{c^{3/2}} \quad (2)$$

where P is the applied load (N), a is the half length of the indent diagonal (m) and c is the median/radial crack length (m). The results quoted are those obtained from the 1.96 N loading due to the higher number of acceptable indentations (a minimum of fifteen per sample).

2.2.3. Aqueous durability assessment

Aqueous durability assessment was performed according to ASTM standard C 1285–02 (Product Consistency Test - PCT) utilising a 75 μm–150 μm size fraction in 18.2 MΩ H_2O at 90 °C with a SA/V between 1499 m^{-1} and 1525 m^{-1} dependent on glass density, as provided in Table 3 [25]. Experiments were performed in triplicate with duplicate blanks, sampling at 3, 7, 14, 21 and 28 days. Samples were filtered using a 0.45 μm PTFE filter and leachate analysis was performed using ICP-AES.

Table 3
Properties of glass wasteforms produced at varying PFR raffinate waste loadings including the density, liquidus temperature (measured in mullite crucibles – see main text for the implication of this) and glass transition temperature.

Glass Property	Sample ID		
	G73-10	G73-15	G73-20
Density (g cm^{-3})	3.512 ± 0.002	3.572 ± 0.002	3.574 ± 0.003
Glass Transition Temperature (°C)	470 ± 10	483 ± 10	484 ± 10
Liquidus Temperature (°C)	1045 ± 10	1075 ± 10	1020 ± 10

The normalised elemental mass loss (NL_i) and normalised elemental dissolution rates (NR_i) were calculated according to Equations (3) and (4), respectively; using the analysed glass compositions.

$$NL_i = \frac{C_i}{f_i \times \frac{SA}{V}} \quad (3)$$

$$NR_i = \frac{C_i}{f_i \times \frac{SA}{V} \times t} \quad (4)$$

where NL_i is the normalised elemental mass loss of element *i* (g m^{-2}), C_i is the averaged, blank corrected concentration of element *i* in solution (g m^{-3}), f_i is the fraction of element *i* in the unleached glass, SA/V is the ratio of glass surface area to the volume of water (m^{-1}), NR_i is the normalised elemental loss rate and t is time in days.

Geochemical modelling of the solution leachate was performed using the PhreeqC geochemical modelling code (v3-12-8538, provided by the United States Geological Survey) to identify solution saturation species, using the Lawrence Livermore National Laboratory (LLNL) thermodynamic database.

3. Results

3.1. Glass formation and composition

It can be stated with confidence that the three simulant PFR waste loaded G73 glasses exist within a stable glass forming region of the phase diagram up to a 20 wt% loading. The glasses formed readily and poured from the melt at 1200 °C, with no evidence of un-dissolved batch. However, a small degree of corrosion was evident inside the crucible, which is responsible for the elevated concentrations of alumina in the final composition. The composition of the three glasses was analysed using XRF and ICP-AES; data are shown in Table 2, which compares the final composition with the nominal batched compositions.

Overall, it can be seen from Table 2 that the batched and analysed compositions are in reasonable agreement for major and minor oxides, although with some notable exceptions. Na_2O, B_2O_3, and SO_3, are, in general, analysed as lower than the batched composition, due to volatilisation from the melts during high temperature processing. SiO_2 and BaO are, respectively, systematically higher and lower in the analysed glass compositions compared to the batched. The complexity of the glass composition made deconvolution of overlapping X-ray emission lines, from multiple elements, challenging and may be responsible for this systematic discrepancy. The loss of volatile components from the melts does not pose a challenge to the off-gas system of existing HLW melter systems and, therefore, is not expected to be problematic for full scale deployment. In addition, it should be noted that the lower surface area to volume ratio, and presence of a cold cap, in full scale melter systems will reduce volatilisation considerably, with respect to laboratory scale melts.

Analysis of the vitrified products by X-ray diffraction showed only diffuse scattering (Fig. 1) characteristic of an amorphous material, with no evidence of phase separation or detectable crystallisation. The lack of contrast in both the SEM-BSE imaging and SEM-EDX mapping analysis, displayed in Figs. 1b and 2, is indicative of a chemically homogeneous glass on a micron scale. Each glass showed similar characteristics. There was no evidence from XRD or SEM-EDX analysis of distinct segregated sulphate phases.

Crystallisation in radioactive waste glasses, when produced from the melt, is undesirable for several reasons, including: the possibility for the precipitation of soluble radionuclide containing phases; the potential for decreased aqueous durability of the matrix, due to the removal of refractory components; and the potential for swelling of crystal phases as a result of damage from self-irradiation. The absence of significant crystallisation and minimal evidence of crucible corrosion indicate that a high-quality glass wasteform was obtained that should be both stable and amenable to the processing of PFR wastes.

3.2. Thermal properties

Table 3 shows the density, glass transition temperature and measured liquidus temperature of the simulant PFR glasses. The values obtained for the T_g are comparable, within error, for the three waste-loadings and correspond well with the transition temperature previously reported for the same base glass loaded with organic exchange resins [18–21].

The liquidus temperatures of the glasses were all below 1100 °C, and no correlation with increasing waste loading was observed. Glass compositions with a liquidus temperature below 1100 °C are thought to be beneficial for nuclear waste vitrification as the lower temperatures minimise volatile losses of radioactive components during melting [27–29]. Although not essential for all melter operations or wasteform acceptance criteria, the absence of crystalline products indicates that the wasteforms will be amenable to commercial application, due to the associated simplification of wasteform qualification, improved efficiency of melter operation and predictability of process control [30].

As the glasses produced in this study have been shown to retain their Cs inventory after processing at 1200 °C, the retention of Cs should be expected to be retained in full scale melts given the smaller melt surface area to volume ratio and possibility of operating with a cold cap [31].

3.3. Mechanical testing

The Vickers hardness and indentation fracture toughness of the PFR simulant glasses are plotted in Fig. 3. The fracture toughness of the glass relates to the energy required to form a new surface and is relevant to qualifying the suitability of radioactive waste packages for transport, e.g. in estimating the likelihood of respirable fines formation in accident scenario [32].

The lowest waste loaded glass, G73-10, had the highest indentation fracture toughness and the hardness value of the glasses

tested. G73-15 and G73-20 glasses gave lower values and were equivalent within measurable precision. All compositions were comparable or superior to existing HLW glass compositions (e.g. UK MW glass and US PNL 76–78 glass, Fig. 3) for indentation fracture toughness and were comparable, or superior, in terms of Vickers hardness [26,32].

Although no specification for fracture toughness currently exists for UK vitreous waste packages, the results imply that, as the G73 based glasses are comparable to current wasteforms, they are likely to be compliant with storage in existing (HLW) canisters. Furthermore, the mechanical properties suggest that packaging in larger 3 m^3 boxes may also be possible, although in this case analysis of thermally induced cracking/stresses during processing requires investigation.

3.4. Aqueous durability

The short-term chemical durability of the simulant raffinate glasses was investigated using the PCT methodology [25]. Fig. 4 shows the normalised mass loss of elements that were detectable by ICP-AES in concentrations higher than those measured in the blank solutions. The normalised elemental mass loss (NL_i) and normalised dissolution rate (NR_i, 28 days) data are shown in Tables 4 and 5, respectively. The solution pH buffered to a value of pH 10.2 ± 0.2 after 3 days (Fig. 4) and there was no further measurable fluctuation of pH during the 28-day duration of the experiments.

The normalised mass loss rates (to 28 days) for boron were similar for each glass composition, giving an NR_B between 3.24×10^{-2} g m^{-2} d^{-1} and 3.33×10^{-2} g m^{-2} d^{-1} ($\pm 5 \times 10^{-4}$) as stated in Table 4. This indicates that varying the waste loading from 10 to 20 wt% did not appreciably alter the chemical durability on the timescales investigated. Importantly, the glasses showed a comparable normalised mass loss and normalised dissolution rate to other high-level waste glass compositions destined for long-term disposal, tested under comparable conditions (Table 5). For example, the UK HLW MW25 glass, has a NR_B of 3.20×10^{-1} g m^{-2} day^{-1} [33], compared with 3.24×10^{-2} g m^{-2} d^{-1} for the 20 wt% loaded simulant PFR raffinate glass (Table 5). The NR_B is approximately twice that of the SON68 French HLW base glass, however it should be noted that the specific activity in R7T7 (the active analogue of SON68) will be substantially higher than that of the PFR loaded G73 glasses. At production, R7T7 contains an average specific activity ca. 110 PBq m^{-3}, approximately 20 times greater than the average ca. 6 PBq m^{-3} estimated for the G73-20 glass [34]. As such, these glasses could be considered suitable for the immobilisation and disposal of PFR raffinate.

Glass dissolution was observed to be incongruent; B and Na leached at similar rates ($NL_B > NL_{Na}$), however the normalised mass loss of all other elements was an order of magnitude lower than both B and Na (Table 4). The normalised mass loss of all elements was observed to be rapid for the first 3 days of dissolution and, after this time, the normalised mass loss of Si, Na, B began to reduce indicating an approach to quasi-equilibrium, as indicated in Fig. 4.

The normalised mass loss of Ba and Ca differed as a function of glass composition, albeit without a notable trend. For example, the normalised mass loss of Ba decreased after 7 days for the 20 wt% waste loaded composition, and after 14 days for the 15 wt% glass (Fig. 4b). There appeared to be little removal of Ba from solution from the 10 wt% loaded glass. Additionally, the NL_{Sr} dropped after 14 days for all three glasses (Fig. 4f). This behaviour may be attributed to the formation of Ca-, Ba- and Sr-containing alteration layers on the glass surface. Indeed, geochemical modelling indicated that tobermorite ($Ca_5Si_6H_{11}O_{22.5}$) is likely to precipitate. A number of recent investigations have also identified this phase in glasses containing Ca, or where Ca is present in solution [35–39] and have shown that its formation can significantly reduce the dissolution rate of nuclear waste glasses, by an order of magnitude compared to other media [39]. Other phases shown by geochemical modelling to be favourable precipitates were the Ca- Ba- and Sr-

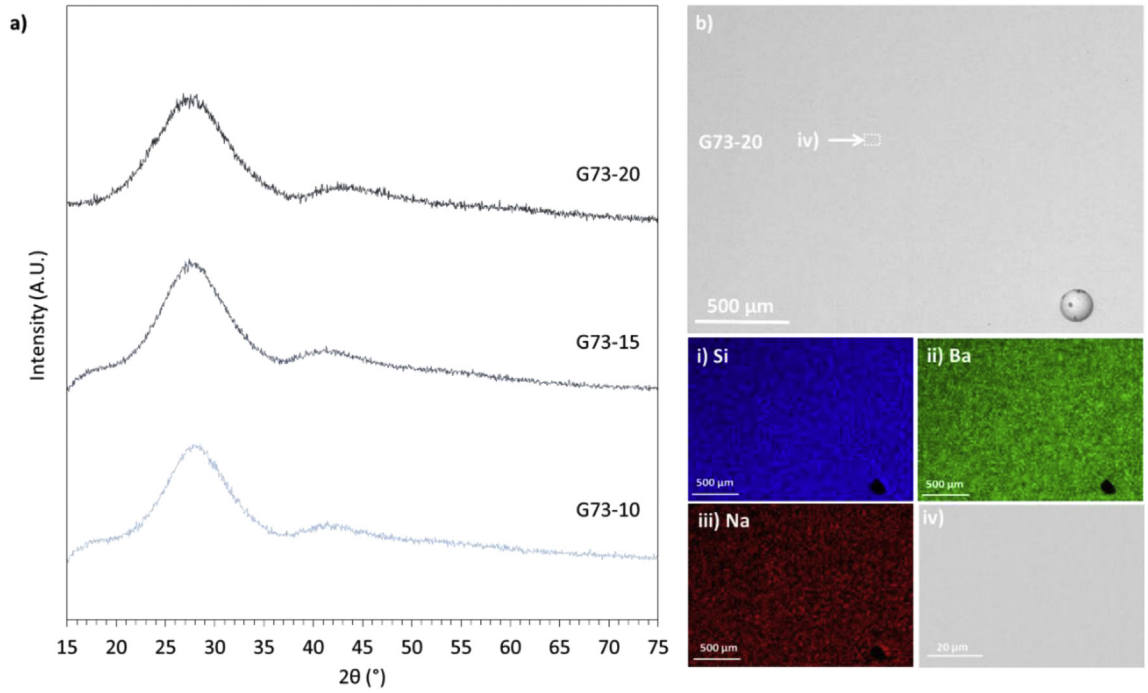

Fig. 1. A) Powder XRD patterns of G73 PFR raffinate loaded glasses, displaying diffuse scattering characteristic of amorphous material and b) SEM-BSE image displaying homogeneity of G73-20 glass matrix, set above i) - iii) SEM-EDX maps of key elements for b) and iv) a higher resolution BSE-SEM of G73-20 glass matrix identified in b) which taken illustrates the absence of crystalline materials in the final waste product.

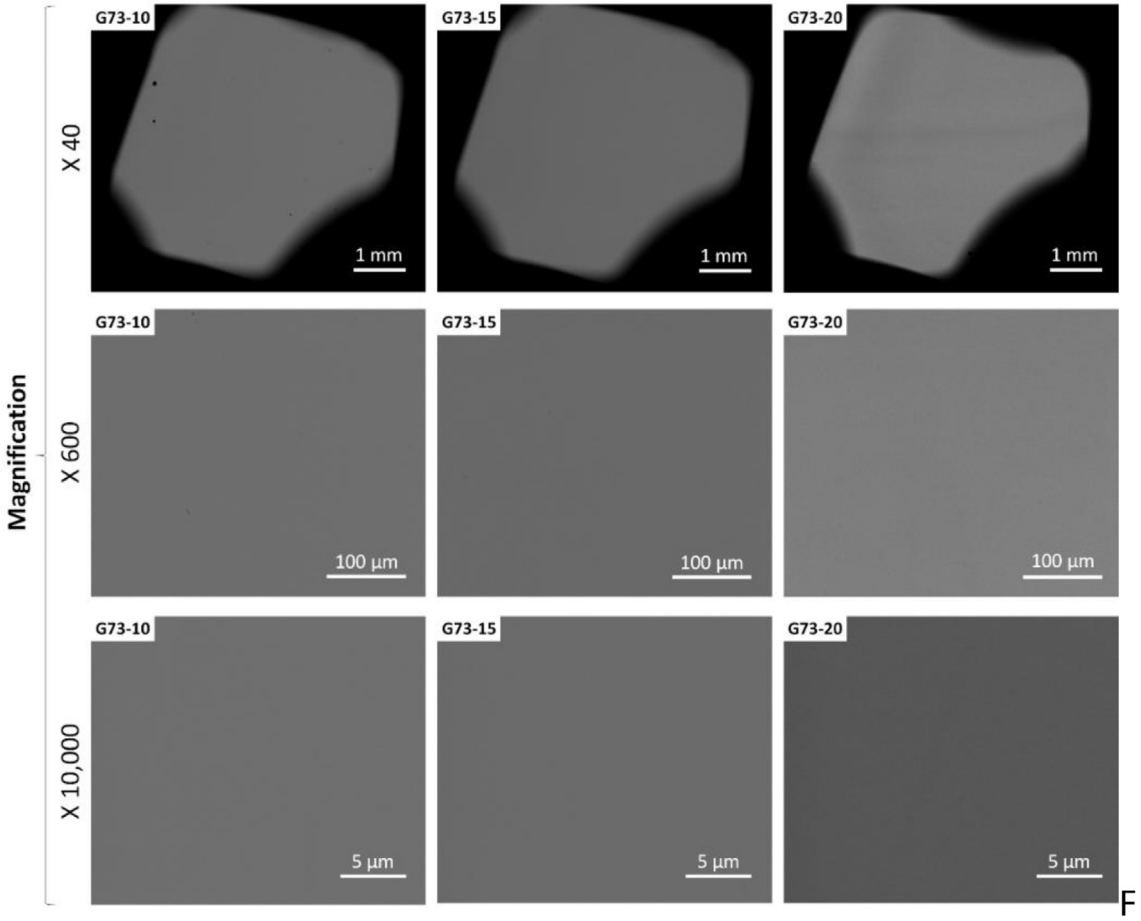

Fig. 2. SEM-BSE images of the three waste loaded glasses G73-10, G73-15 and G73-20 at various magnifications. The lack of image contrast suggests chemical homogeneity within the sample.

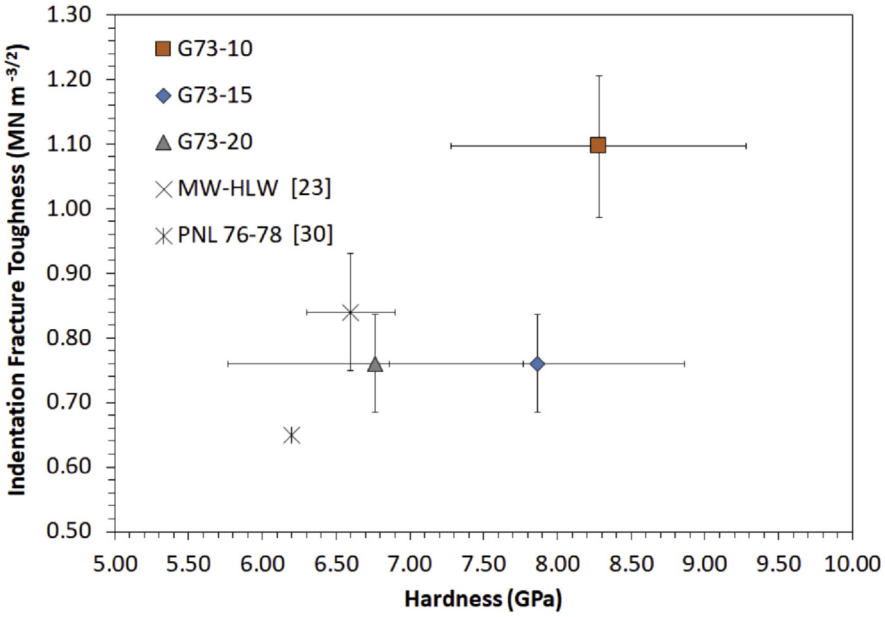

Fig. 3. Indentation fracture toughness and hardness values of G73 PFR raffinate waste loaded glasses obtained using the Vickers indentation methodology, with comparison to waste glasses currently used for HLW immobilisation [23,30]. Errors correspond to 3 x the measured standard deviation.

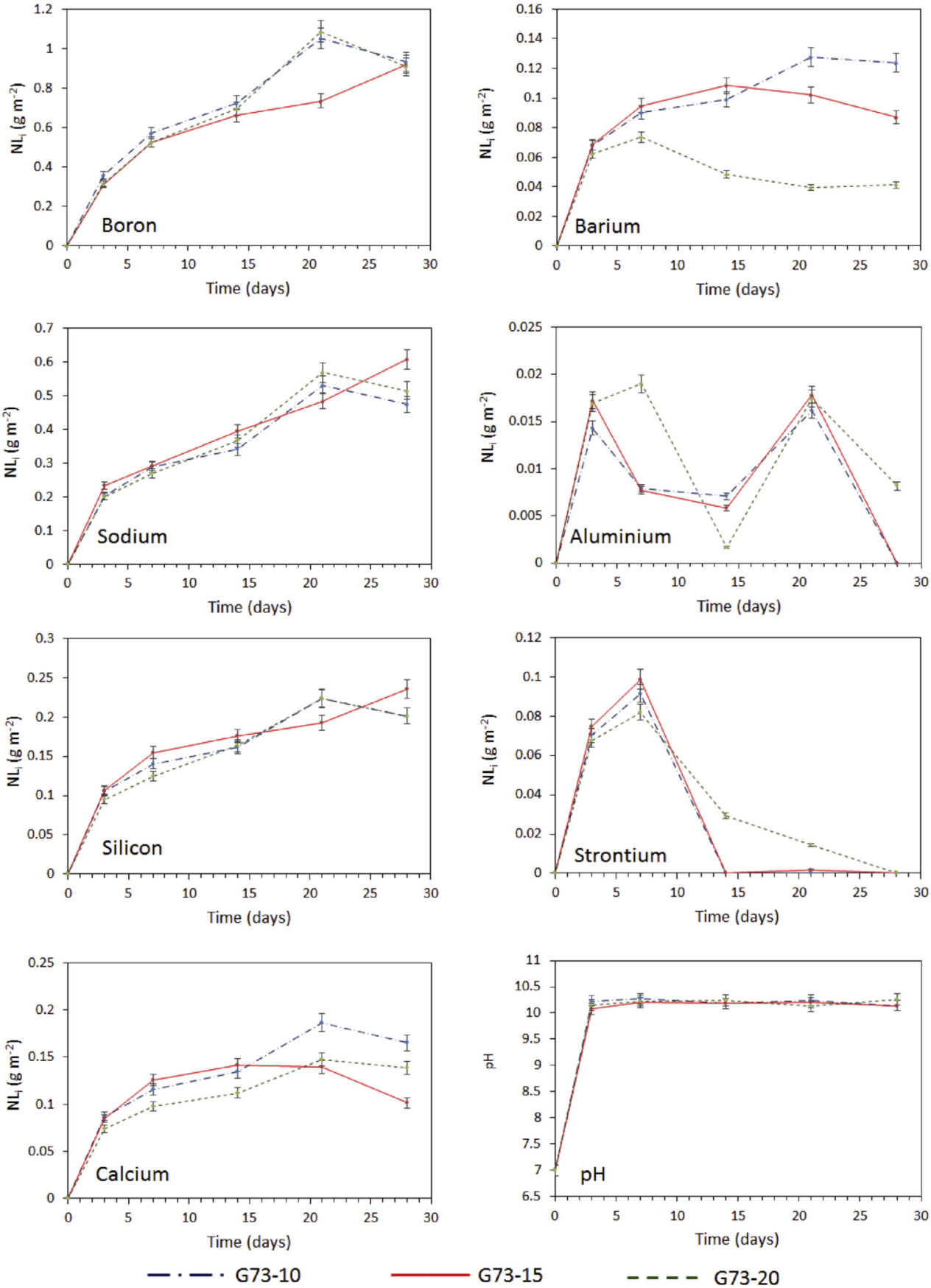

Fig. 4. Graphs displaying the normalised elemental mass loss with varying levels of PFR raffinate loading from PCT experiments at 90 °C in 18.2 MΩ water with a SA/V of 1499 m^{-1} -1525 m^{-1} (dependant on glass density).

carbonate phases, calcite ($CaCO_3$), witherite ($BaCO_3$) and strontianite ($SrCO_3$). Arising from equilibrium of CO_2 in air with the leaching medium, it is possible that these phases precipitated in solution, and when the samples were filtered for analysis, they were removed, leading to an apparent decrease in Ca, Ba and Sr leaching. It will be necessary to perform further monolith leaching experiments to examine the properties of the altered layer so that the origin of the fluctuations in these elements can be determined and set in the context of recent mechanistic studies of UK HLW and ILW glass performance [40–43].

4. Discussion

Previous work has shown that cement may not have the capacity to effectively immobilise the diverse inventory of radioactive elements present in the PFR raffinate waste stream [44]. Cementitious wasteforms could be subject to increased dissolution and release rates due to their inherent porosity and high internal surface area. The high solubility and potential for removal of many of the waste elements which sorb to the cement surface; especially Cs, which makes up over 60% of the radioactive inventory by activity, is of potential concern [2]. These factors highlight the opportunity to vitrify PFR wastes to minimise radioisotope migration to the biosphere. Vitrification, using G73 barium silicate glass described in this investigation, is likely to offer significant improvements in long term wasteform performance over the current baseline.

The benefits of vitrification reach beyond the improvements in wasteform quality described and may also offer fiscal incentives, for example, by substantially reducing the waste volumes for storage and disposal. The current lifecycle waste management plan is to cement the PFR raffinate in 500 L drums, with a target waste loading of 0.305 m^3 per drum. With 212.1 m^3 of raffinate to process this would result in 397 m^3 of packaged waste for disposal (696 × 500 L drums with a displacement volume of 0.57 m^3 each) [2]. If vitrification, at 20 wt% loading was to be utilised, the volume of waste produced would be reduced to <14.4 m^3 of glass. Conceivably, this volume of material could be readily processed in a small or modular plant, utilising one of a variety of thermal treatment options for ILW being developed in the UK e.g. plasma vitrification, resistive heating melters or Hot-Isostatic Pressing [45].

Assuming packaging of vitrified PFR waste into 3 m^3 ILW boxes was preferable and 70% of the box capacity (2.57 m^3) could be filled, each 3 m^3 box would hold 1.8 m^3 of vitrified product. In this scenario, the waste could be fully conditioned using just eight 3 m^3 boxes, producing a total waste volume for disposal of 28.6 m^3. This treatment methodology, when compared with cementation, would reduce the waste disposal inventory by more than 90%, and, in principle, could be achieved, using in-container Joule heated melter technology. The heat generation, surface activity limits and containment limits for impact of this hypothetical G73-20 waste stream have been estimated to be within existing guidelines for a 3 m^3 ILW box[1] [46]. The substantial volume reduction achieved by the vitrification approach would enable transfer of the resulting waste packages to the Sellafield site for storage, potentially assisting earlier closure of the Dounreay site.

Deriving a lifetime waste management cost for these wastes intended for near surface storage has not been attempted here. However, it is believed the cost reductions associated with managing lower volumes of wastes in the rest of the NDA estate should be transferable to Scottish policy. It is important to note that the volume reduction and concentration of the waste associated with this vitrification step would not result in the re-classification of the waste as HLW. This is important as a reclassification to HLW would require consideration of heat dissipation in storage, introducing significant extra costs for disposal, as well as increasing the final volume required in a storage vault.

The decreased risk to public health, superior quality of final wasteform, improved long term stability, smaller footprint on the Dounreay ILW stores and the reduced waste management cost, combine to provide a credible case for treatment of these wastes using vitrification over cementation.

[1] Calculation based upon reported inventory of radioisotopes for this waste stream and accounting for the concentration of activity achieved by vitrification. This packaged waste will meet stated specifications imposed for a square corner 3 m^3 box.

Table 4
Normalised elemental loss rates for the three waste PFR waste loaded glasses measured after 28 days. Data is from PCT experiments of the wasteforms at 90 °C in 18.2 MΩ water.

NR_i (g m^{-2} day^{-1})	Glass Composition		
	G73-10	G73-15	G73-20
B	3.33×10^{-2}	3.28×10^{-2}	3.24×10^{-2}
Na	1.69×10^{-2}	2.17×10^{-2}	1.84×10^{-2}
Si	7.18×10^{-3}	8.40×10^{-3}	7.19×10^{-3}
Ca	5.89×10^{-3}	3.62×10^{-3}	4.95×10^{-3}
Mo	4.44×10^{-3}	4.78×10^{-3}	6.38×10^{-3}
Ba	4.43×10^{-3}	3.10×10^{-3}	1.47×10^{-3}
Cr	3.48×10^{-4}	1.64×10^{-4}	2.30×10^{-4}
Cu	4.93×10^{-6}	1.45×10^{-6}	0.00
Al	0.00	0.00	2.91×10^{-4}
Fe	0.00	0.00	0.00
Ni	0.00	0.00	0.00
Sr	0.00	0.00	0.00
Zn	0.00	0.00	0.00

Table 5
Comparison of network dissolution limiting normalised elemental mass losses and normalised elemental dissolution rates between SON68 glass, British Magnox waste HLW glass and G73-15 waste loaded glasses tested, under PCT conditions at 90 °C in 18.2 MΩ water.

Glass Composition	NL_i after 28 days (g m^{-2})		NR_i after 28 days (g m^2 day^{-1})		SA/V (m^{-1})	pH (25 °C)
	NL_B	NL_{Si}	NR_B	NR_{Si}		
G73-20	0.9076	0.2012	0.0324	0.0072	1499	10.26
SON68 [40]	0.4886	0.1559	0.0175	0.0055	2135	9.4
MW25 [31]	8.89	0.538	0.32	0.020	1200	–

5. Conclusion

A vitreous wasteform for simulant PFR raffinate was developed at a range of waste loadings up to 20 wt%. The product was a stable and homogeneous amorphous solid with no observable crystal formation. All glasses performed comparably to vitrified waste compositions currently in use, both in the UK and internationally, for the immobilisation of HLW. The aqueous durability was superior to that of current UK HLW glasses under comparable experimental conditions. Therefore, the glasses investigated here could be considered a stable matrix for ILW under both geological disposal and near-surface storage scenarios. The mechanical properties of the wasteform also matched or exceeded those currently in use for HLW glasses, in both the UK and USA, and therefore, should be amenable to transport and storage in either 500 L HLW flasks or 3 m^3 ILW waste packages. Additionally, we demonstrated that undertaking immobilisation of PFR raffinate through thermal treatment methods may also result in a decrease in the anticipated volume of waste from 397 m^3 to 28.6 m^3, potentially resulting in significant lifetime waste management cost savings and a more

robust option to support the Scottish policy for at near surface storage and site closure.

Acknowledgements

The authors would like to thank Paul Lythgoe and Alastair Bewsher (School of Earth Science, University of Manchester) for performing the XRF and ICP-AES measurements presented in this work, Martina Klinkenberg and Jülich Forshungszentrum for access to the FEI SEM. This research was performed in part at the MIDAS Facility, at the University of Sheffield, which was established with support from the Department of Energy and Climate Change. We are grateful to EPSRC for sponsorship of this research under grants EP/G037140/1, EP/N017870/1, and EP/N017374/1.

References

[1] S.E. Jensen, P.L. Ølgaard, Description of the Prototype Fast Reactor at Dounreay, NKS/RAK-2(95)TR-c 1, Rise National Laboratory, Roskilde, Denmark, NKS, 1996. http://www.iaea.org/inis/collection/NCLCollectionStore/_Public/28/026/28026107.pdf. (Accessed 7 January 2017).
[2] Nuclear Decommissioning Authority, Waste Stream 5B01-PFR Raffinate, UK Radioactive Waste Inventory, 2014.
[3] K.F. Langley, B.A. Partridge, M. Wise, Immobilization of fast reactor first cycle raffinate, in: Proceedings of Waste Management - Tuscon AZ, 2003. http://www.wmsym.org/archives/2003/pdfs/50.pdf. (Accessed 7 January 2017).
[4] United Kingdom Atomic Energy Authority (UKAEA), Justification for Classifying PFR Raffinate as ILW, DSRPTC, 2003, p. P11, 2003.
[5] United Kingdom Atomic Energy Authority (UKAEA), How to Deal with the Management of Prototype Fast Reactor (PFR) Raffinate, UKAEA/PP/P, 2004, p. 01, 2004.
[6] United Kingdom Atomic Energy Authority (UKAEA), Best Practicable Environmental Option Study for the Management of PFR Raffinate, 2005. D3900(04)P027.
[7] Nuclear Decommissioning Authority, Waste Stream 5B04-MTR Raffinate, UK Radioactive Waste Inventory, 2014.
[8] Nuclear Decommissioning Authority, Waste Stream 5B05-DFR Raffinate, UK Radioactive Waste Inventory, 2014.
[9] J.H. Sharp, J. Hill, N.B. Milestone, E.W. Miller, Cementitious systems for encapsulation of intermediate level waste, in: Proceedings of ICEM '03: the 9th International Conference on Radioactive Waste Management and Environmental Remediation, Oxford, UK, 2003.
[10] F.P. Glasser, Mineralogical aspects of cement in radioactive waste disposal, Mineral. Mag. 65 (2001) 621–633.
[11] N.B. Milestone, Y. Bai, C.H. Yang, X.C. Li, The use of activated slags as immobilisation matrices for ILW, in: MRS Online Proceedings Library, vol. 1107, 2008.
[12] Committee on Radioactive Waste Management (CoRWM), Response to Scotland's Policy on Higher Activity Radioactive Waste: Consultation on an Implementation Strategy, CoRWM Document .3220, 2015.
[13] Scottish Government, Consultation on an Implementation Strategy for Scotland's Policy on Higher Activity Radioactive Waste, 2015.
[14] E.R. Merz, D. Dyckerhoff, R. Odoj, Characterization of radioactive wastes incorporated in a cement matrix, in: Proceedings of International Conference on Radioactive Waste Management, 1986, pp. 396–401.
[15] H.J. Mockel, R.H. Koster, Gas Formation during the Gamma Radiolysis of Cemented Low-and Intermediate-level Waste Products, NT, vol. 59, 1982, pp. 494–497.
[16] N.E. Bibler, Radiolytic Gas Production from Concrete Containing Savannah River Plant Waste, Du Pont de Nemours (E.I.) and Co, 1978. http://inis.iaea.org/Search/search.aspx?orig_q=RN:9389931. (Accessed 9 February 2017).
[17] C.A. Utton, I.H. Godfrey, Review of Stability of Cemented Grouted Ion-Exchange Materials, Sludges and Flocs, vol. 212, NNL(09) 10, January, 2010. Issue 2, https://rwm.nda.gov.uk/publication/review-of-stability-of-cemented-grouted-ion-exchange-materials-sludges-and-flocs-january-2010/. Accessed 9 February 2017.
[18] P.A. Bingham, N.C. Hyatt, R.J. Hand, C.R. Wilding, P.A. Bingham, N.C. Hyatt, R.J. Hand, C.R. Wilding, Glass development for vitrification of wet intermediate level waste (WILW) from decommissioning of the Hinkley point 'a' site, in: MRS Online Proceedings Library, vol. 1124, 2008, pp. Q03–Q07.
[19] P.A. Bingham, N.C. Hyatt, R.J. Hand, Vitrification of UK intermediate level radioactive wastes arising from site decommissioning: property modelling and selection of candidate host glass compositions, Glass Technol. Eur. J. Glass Sci. Technol. 53 (2012) 83–100.
[20] P.A. Bingham, N.C. Hyatt, R.J. Hand, S.D. Forder, Vitrification of UK intermediate level radioactive wastes arising from site decommissioning. initial laboratory trials, Glass Technol. Eur. J. Glass Sci. Technol. 54 (2013) 1–19.
[21] O.J. McGann, P.A. Bingham, R.J. Hand, A.S. Gandy, M. Kavcic, M. Zitnik, K. Bucar, R. Edge, N.C. Hyatt, The effects of γ-radiation on model vitreous wasteforms intended for the disposal of intermediate and high level radioactive wastes in the United Kingdom, J. Nucl. Mater. 429 (2012) 353–367.
[22] C.P. Kaushik, R.K. Mishra, P. Sengupta, A. Kumar, D. Das, G.B. Kale, K. Raj, Barium borosilicate glass – a potential matrix for immobilization of sulfate bearing high-level radioactive liquid waste, J. Nucl. Mater. 358 (2006) 129–138.
[23] B. Brendebach, M.A. Denecke, G. Roth, S. Weisenburger, Sulfur incorporation in high level nuclear waste glass: a S K-edge XAFS investigation, J. Phys.: Conf. Ser 190 (2009), 012186.
[24] C.H. Oh, Hazardous and Radioactive Waste Treatment Technologies Handbook, CRC Press, 2001.
[25] C 1285–02 Standard Test Methods for Determining Chemical Durability of Nuclear, Hazardous, and Mixed Waste Glasses and Multiphase Glass Ceramics: the Product Consistency Test (PCT), ASTM International, 2008.
[26] A.J. Connelly, R.J. Hand, P.A. Bingham, N.C. Hyatt, Mechanical properties of nuclear waste glasses, J. Nucl. Mater. 408 (2011) 188–193.
[27] M. Asano, T. Kou, Y. Mizutani, Vaporization of alkali borosilicate glasses, J. Non-Cryst. Solids 112 (1989) 381–384.
[28] B.G. Parkinson, Influence of Composition on Structure and Caesium Volatilisation from Glasses for HLW Confinement, The University of Warwick, 2007.
[29] J.E. Shelby, An Introduction to Glass Science and Technology, second ed., The Royal Society of Chemistry, Cambridge, 2005.
[30] R. Short, Phase separation and crystallisation in UK HLW vitrified products, Procedia Materials Science 7 (2014) 93–100, https://doi.org/10.1016/j.mspro.2014.10.013.
[31] M.H. Langowski, J.G. Darab, P.A. Smith, Volatility Literature of Chlorine, Iodine, Cesium, Strontium, Technetium, and Rhenium; Technetium and Rhenium Volatility Testing, Pacific Northwest Lab, 1996. http://inis.iaea.org/Search/search.aspx?orig_q=RN:27054276. (Accessed 13 January 2017).
[32] I.W. Donald, B.L. Metcalfe, R.N.J. Taylor, The immobilization of high level radioactive wastes using ceramics and glasses, J. Mater. Sci. 32 (1997) 5851–5887.
[33] H.U. Zwicky, B. Grambow, C. Magrabi, E.T. Aerne, Corrosion behaviour of British Magnox waste glass in pure water, MRS Online Proc. Libr. 127 (1988) 127–129.
[34] L. Wang, Advances in Transport Phenomena, Springer Science & Business Media, 2009.
[35] C.A. Utton, R.J. Hand, N.C. Hyatt, S.W. Swanton, S.J. Williams, Formation of alteration products during dissolution of vitrified ILW in a high-pH calcium-rich solution, J. Nucl. Mater. 4421 (2013) 33–45.
[36] S. Mercado-Depierre, F. Angeli, F. Frizon, S. Gin, Antagonistic effects of calcium on borosilicate glass alteration, J. Nucl. Mater. 441 (2013) 402–410.
[37] S. Gin, P. Jollivet, M. Fournier, C. Berthon, Z. Wang, A. Mirtoshkov, Z. Zhu, J.V. Ryan, The fate of silicon during glass corrosion under alkaline conditions: a mechanistic and kinetic study with the International Simple Glass, Geochem. Cosmochim. Acta 151 (2015) 68–85.
[38] C.A. Utton, S.W. Swanton, J. Schofield, R.J. Hand, A. Clacher, N.C. Hyatt, Chemical durability of vitrified wasteforms: effects of pH and solution, Mineral. Mag. 76 (2012) 2919–2930.
[39] C.L. Corkhill, N.J. Cassingham, P.G. Heath, N.C. Hyatt, Dissolution of UK high level waste glass under simulated hyperalkaline conditions of a co-located geological disposal facility, Int. J. Appl. Glass Sci. 4 (2013) 341–356.
[40] N. Cassingham, C.L. Corkhill, D.J. Backhouse, R.J. Hand, J.V. Ryan, J.D. Vienna, N.C. Hyatt, The initial dissolution rates of simulated UK Magnox-THORP blend nuclear waste glass as a function of pH, temperature and waste loading, Mineral. Mag. 79 (2015) 1529–1542.
[41] H. Zhang, C.L. Corkhill, P.G. Heath, R.J. Hand, M.C. Stennett, N.C. Hyatt, Effect of Zn- and Ca oxides on the structure and chemical durability of simulant alkali borosilicate glasses for immobilisation of UK high level wastes, J. Nucl. Mater. 462 (2015) 321–328.
[42] N.J. Cassingham, C.L. Corkhill, M.C. Stennett, R.J. Hand, Alteration layer formation of Ca- and Zn-oxide bearing alkali borosilicate glasses for immobilisation of UK high level waste: a vapour hydration study, J. Nucl. Mater. 479 (2016) 639–646.
[43] N.C. Hyatt, R.R. Schwarz, P.A. Bingham, M.C. Stennett, M.C.C.L. Corkhill, P.G. Heath, R.J. Hand, M. James, A. Pearson, S. Morgan, Thermal treatment of simulant plutonium contaminated materials from the Sellafield site by vitrification in a blast-furnace slag, J. Nucl. Mater. 444 (2014) 186–199.
[44] M. Atkins, F.P. Glasser, Application of Portland cement-based materials to radioactive waste immobilization, Waste Manag. 12 (1992) 105–131.
[45] N.C. Hyatt, M. James, Thermal treatment of ILW, Nucl. Eng. Int. 58 (2013) 10–13.
[46] G. Steele, Areva Risk Management Consulting, Contents Activity for the Square Corner 3 M^3 Box Waste Package Transported in an SWTC-285 Transport Container, NDA.RWMD, 2009, pp. R07–R023 (C) J6214.23.